

INFLUENCE OF SELECTED PARAMETERS ON ASH PARTICLE TRAJECTORIES WHEN MODELLING DEPOSITION ON SUPERHEATER TUBES IN PULVERISED COAL BOILERS USING FLUENT CODE

Krzysztof Waclawiak^{1*}, Sylwester Kalisz²

¹Silesian University of Technology, Department of Industrial Informatics, ul. Krasińskiego 8, 40-019 Katowice, Poland

²Silesian University of Technology, Institute of Power Engineering and Turbomachinery, ul. Konarskiego 18, 44-101 Gliwice, Poland

Widely used CFD codes enable modelling of PC boilers operation. One of the areas where these numerical simulations are especially promising is predicting deposition on heat transfer surfaces, mostly superheaters. The basic goal of all simulations is to determine trajectories of ash particles in the vicinity of superheater tubes. It results in finding where on the surface the tube will be hit by particles, and what diameter and mass flow of the particles are. This paper presents results of CFD simulations for a single tube and a bundle of in-line tubes as well. It has been shown that available parameters like ash particle density, shape factor, reflection coefficients affect the trajectories in a different way. All the simulations were carried out with Fluent code of Ansys software.

Keywords: numerical simulation, ash particles, trajectories, superheaters

1. INTRODUCTION

Deposits in power boilers are formed during combustion of practically all solid fuels. The source of deposit formation in boilers is the presence of mineral substance in the fuel. A mineral substance undergoes a series of physical and chemical processes. They produce particles of ash and volatiles which mix with the flue gas. Ash particles floating in the flue gas strike heat exchange surfaces. Steam superheater tubes in power boilers are covered either with powdery deposits, loosely staying on the surface, or bonded ones, stuck firmly onto the surface. The spacing of boiler tubes influences the velocity field of the flue gas and trajectories of ash particles. Orłowski (1972) summarised, for Polish boilers, the tube arrangements of convective in-line superheaters as $s_1/D=1.5-2$ and $s_2/D=1.5-3$, and radiant ones as $s_1=350-1500$ mm, and $s_2/D=1.05-1.1$, where s_1, s_2 - describe tube spacing, and D is a tube diameter. Particles of ash have a size distribution of a few microns up to 200 μm . Typical range of flow velocity within superheater bundles is 5-15 m/s. Typical temperature of flue gas in this area is between 500 and 1000°C. As can be seen, the spacing of tubes and particle size produce quite different conditions resulting in the various history of deposit formation. In two of the latest publications Weber et al. (2013) described prediction of ash particle trajectories using contemporary Computational Fluid Dynamics software. They studied what conditions must be provided in order to predict impaction of ash particles using Reynolds Averaged Navier-Stokes (RANSs) approach. They pointed out that although

*Corresponding author, e-mail: krzysztof.waclawiak@polsl.pl

cpe.czasopisma.pan.pl; degruyter.com/view/j/cpe

the software allows for the prediction, one must be careful not to overestimate the results. Solving particle trajectories should help to predict deposition phenomenon in boilers. Basically, the deposits vary in terms of structure, shape, and temperature of forming. Without going into details fouling deposits can be bonded, powder or sticky. Deposition modelling mostly leads to indication of zones where fouling is likely to happen, by showing areas where ash particles strike the heat transfer surfaces. However, more complicated simulations, when deposition growth model is chosen, result in predictions of deposit shape. Waclawiak and Kalisz (2012) modelled powder deposits on heaters and superheater tubes, and the results were shown for real bundles of tubes in coal-fired boilers, or for a single tube by Waclawiak (2010). Waclawiak and Kalisz (2010) modelled sticky deposition as well. Tomeczek and Waclawiak (2009) showed results from numerical simulations of bonded deposit formation including shape predictions. Most of published materials focus on the deposition rate for heat transfer surfaces without considering deposits already formed onto them. In such cases only trajectories are required to indicate zones in boilers where the deposition is the most likely. Some other examples of using CFD codes to describe boiler operation and indicate areas where the fouling or slagging is most likely to happen can be found in a range of publications over more than a decade, to name some of them: Epple et al. (2005), Fan et al. (2001), Forstner et al. (2006), Huang et al. (1996), Kaer et al. (2001), Kaer et al. (2006), Lee and Lockwood (1999), Ma et al. (2007), Magda et al. (2011), Mueller et al. (2005), Rushdi et al. (2005), Wang and Harb (1997), Yilmaz and Cliffe (2000). An attempt to describe the whole process, from a coal particle burning to ash particle deposition, with an interesting model of ash particle features can be found in a monograph by Lasurdo (2009).

To sum up, obviously deposition in boilers depends on the arrangement of heat transfer surfaces, either convective or radiant superheater tubes. Before CFD codes era, in case of a flow around a cylinder, a correlation between striking (impaction) efficiency and a Stokes number had been widely used, and was defined by Israel and Rosner (1982):

$$\eta = [1 + b(Stk - a)^{-1} - c(Stk - a)^{-2} + d(Stk - a)^{-3}]^{-1} \quad (1)$$

where: $a=0.125$, $b=1.25$, $c=0.014$ and $d=0.00508$, and a Stokes number defined as:

$$Stk = \frac{\rho_p d_p^2 |w_p|}{9\mu_g D} \psi \quad (2)$$

Although this correlation is correct, its use in CFD modelling is restricted, because in boilers there are tube banks, flow is more complex, and most importantly - growing deposits change the tube perimeter. So the entire streamline curvature are different and the surface roughness as well.

2. ASSUMPTIONS OF MODELLING

The Lagrangian reference frame is used by a CFD code to predict the trajectory of an ash particle by integrating the force balance on the particle: gravity, buoyancy, and drag force. This balance, for the x direction in Cartesian coordinates, is as follows:

$$\frac{dw_p}{dt} = \frac{g_x(\rho_p - \rho_g)}{\rho_p} + F_D \quad (3)$$

The drag force F_D is calculated as follows:

$$F_D = \frac{18\mu_g C_D Re}{\rho_p d_p^2} (w_g - w_p) \quad (4)$$

Relative Reynolds number Re is defined as:

$$\text{Re} = \frac{\rho_g d_p |w_p - w_g|}{\mu_g} \quad (5)$$

The drag coefficient C_D for spherical particles is given by Morsi and Alexander (1972):

$$C_D = a_1 + \frac{a_2}{\text{Re}} + \frac{a_3}{\text{Re}} \quad (6)$$

In the case of non-spherical particles Haider's and Levenspiel's (1989) relation is used:

$$C_D = \frac{24}{\text{Re}}(1 + b_1 \text{Re}^{b_2}) + \frac{b_3 \text{Re}}{b_4 + \text{Re}} \quad (7)$$

where the coefficients b_{1-4} are related to the shape factor.

The shape factor is defined as a ratio of the surface area of a sphere having the same volume as the particle to the actual surface area of the particle:

$$\Phi = \frac{S}{S'} \quad (8)$$

Since the software calculates trajectories of the ash particles, the local differences occur between the mass flow of particles striking the tube surface. In order to compare results of simulations for different parameters, the mass flux (surface integral) of ash particles striking the tube surface was calculated:

$$\dot{m}_p = \sum_i \dot{m}_{p,A,i} A_i \quad (9)$$

In order to carry out the simulations of ash trajectories it was assumed that flue gas is air. The flue gas and ash particles enter the model computational grid with velocity of 10 m/s or 7.5 m/s, and temperature of 1300K (1027 °C). The tube surface temperature was 700K (427 °C). Ash particles have density of 2.2 g/cm³ for most simulations, or 1.65 g/cm³ in order to verify its influence on trajectory predictions. Ash concentration in flue gas was set at 10 g/m³. The model takes into consideration the force of gravity acting along the moving ash particles. The turbulence model of $k-\varepsilon$ was chosen with standard parameters, and at the inlet, the gas had turbulent intensity of 10%. The carried out simulations included a prediction of a two-phase coupled flow, so in the discrete phase model panel the interaction between them was active with 10 iterations of the continuous phase per one discrete phase iteration. While tracking the maximum number of steps was set at 2000 and step length factor of 5. In the single tube and three tube simulations there were 120 tracked particles paths.

3. TRAJECTORIES OF PARTICLES STRIKING A SINGLE HORIZONTAL TUBE

In order to test the trajectories prediction, simulations were done for a single tube of 38 mm in diameter, placed in the flue gas duct with a cross-flow arrangement. In front of the tube a 10 diameter long zone, and behind the tube a 5 diameter zone was provided (Fig. 1).

The following simulations were done:

- spherical particles, with density of 2.2 g/cm³ and velocity of 10 and 7.5 m/s;
- spherical particles, with density lowered by 25% to 1.65 g/cm³ and velocity of 10 and 7.5 m/s;
- non-spherical particles approach with the shape factor from 1 (sphere) to 0.1 and density of 2.2 g/cm³ and velocity of 10 and 7.5 m/s;
- non-spherical particles with the shape factor from 1 (sphere) to 0.1 and density of 1.65 g/cm³ and velocity of 10 and 7.5 m/s;
- particles with normal restitution coefficient from 0.0 to 0.9 and density of 2.2 g/cm³, and velocity of 10 m/s;

- spherical particles with tangent restitution coefficient from 0.0 to 0.9 and density of 2.2 g/cm³, and velocity of 10 m/s.

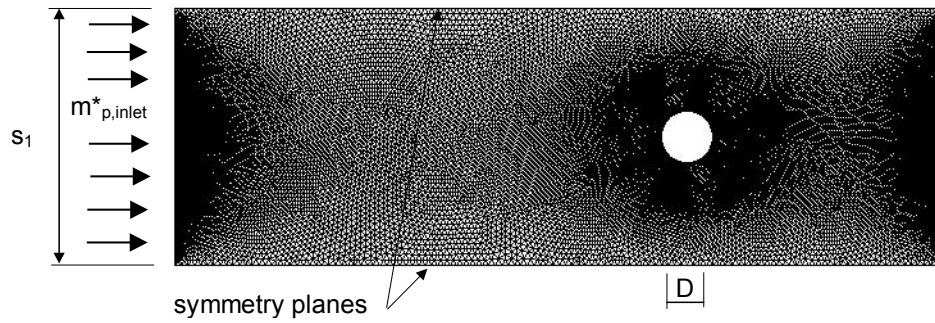


Fig. 1. Computational grid for a single tube simulations

The results from all the simulations were shown in figures Figs. 2 and 3, where striking efficiency was calculated as follows:

$$\eta_{imp} = \frac{\sum \dot{m}_{p,i} A_i}{\dot{m}_{p,inlet} \frac{D}{S_1}} \quad (10)$$

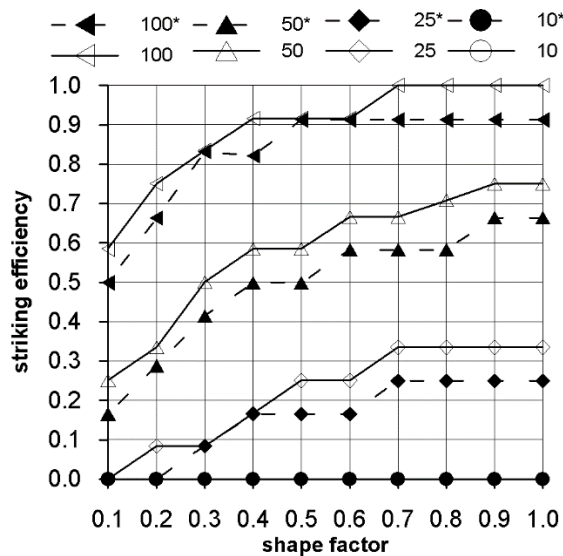


Fig. 2. Effect on striking efficiency of shape factor for different particle diameter (μm), particle density of 2.2 g/cm³, velocity of 10 m/s or 7.5 m/s (*)

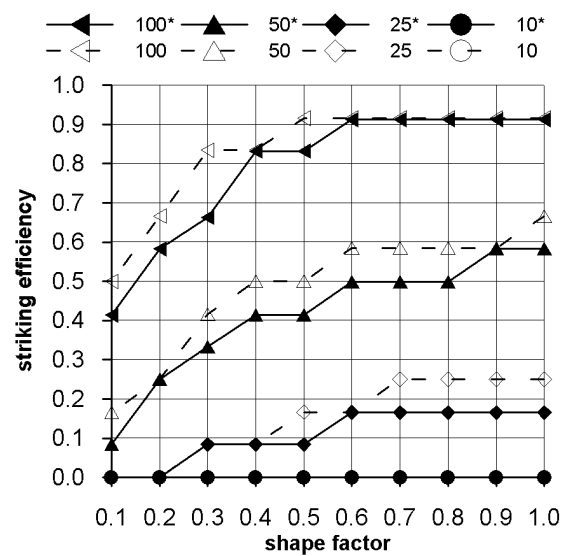


Fig. 3. Effect on striking efficiency of shape factor for different particle diameter (μm), particle density of 1.65 g/cm³, velocity of 10 m/s or 7.5 m/s (*)

As can be seen, the substantial changes in the striking efficiency play a role for particles larger than 10 μm . The drop can reach 50% for larger particles (100 microns) or even 100% for finer particles (25 μm). In case of the finest studied particles they do not strike the tube surface at all. Lowering the velocity of ash particles by 25% results in decreasing the striking efficiency by about 10-15%.

In the case of a single tube in a cross flow of the flue gas only shape factor and density are parameters which can be easily changed. The density and shape factor of ash particles depend on the mineral matter of the fuel, while the shape factor depends on milling process as well. It is reported that biomass ashes often are columnar, an example of this can be found in an article by Yang et al. (2008) with the

factor of 0.78. As was shown in the simulations, this value affects the predicted trajectories of ash particles.

Another couple of parameters which affect the simulations are normal and tangent restitution coefficients. One of available boundary conditions for particles in Fluent code is “reflect”, when the particles rebound off the boundary. The momentum change resulting from the impact is defined by coefficients of restitution: normal and tangent as follows:

$$e_{normal} = \frac{W_{p2,normal}}{W_{p1,normal}} \quad (11)$$

$$e_{tangent} = \frac{W_{p2,tangent}}{W_{p1,tangent}} \quad (12)$$

When a normal or tangent restitution coefficient is equal to 1 it describes an elastic collision when the particles retain all of their momentum. On the contrary to the elastic collision, particles lose their momentum after collision when their restitution coefficients are equal to zero. Basically in the case of the chosen layout (Fig. 1), where a major component of the velocity is normal to the surface for most particles and flow parameters the tangent restitution coefficient does not affect the striking efficiency at all. In case of the normal restitution coefficient the change is not substantial and can be observed for larger particles. It is interesting that in the case of non-elastic collision some particles strike the tube twice. These multi-impact leads to increase in the striking efficiency to the values greater than 1.0. In order to have a better understanding of the change in trajectory during the simulated impact some close-ups have been shown in Figs. 4 and 5.

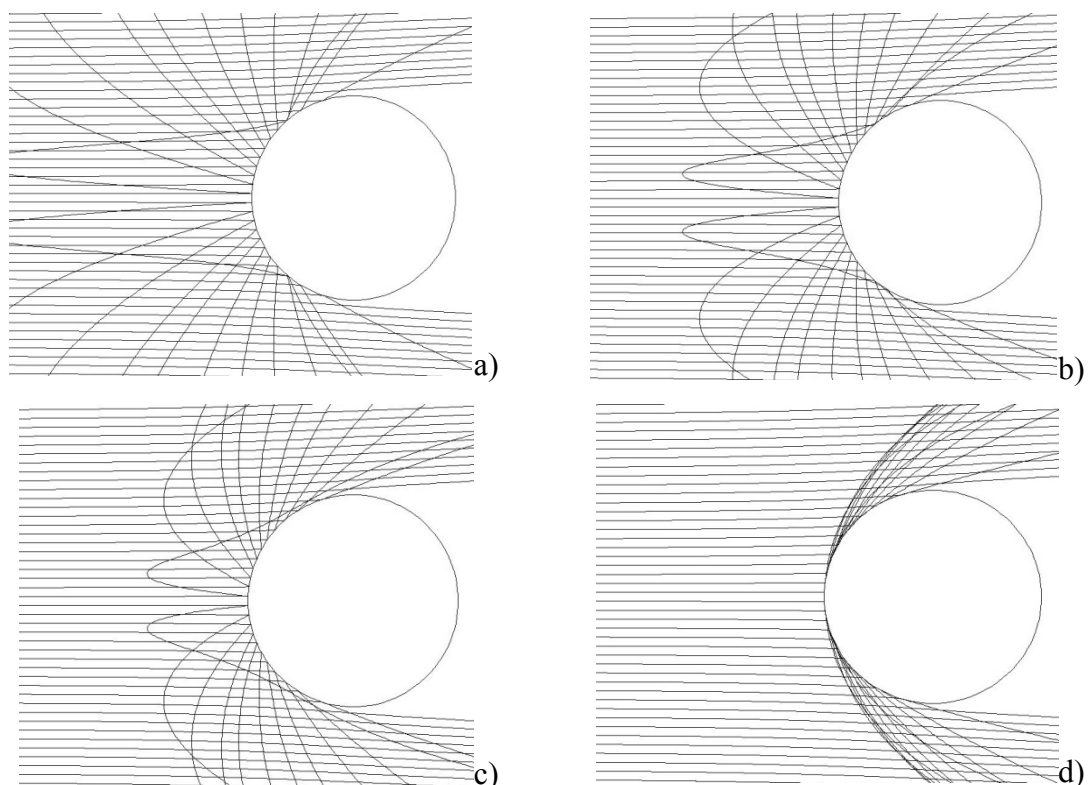


Fig. 4. Simulated trajectory for particles of 100 μm in diameter when they are spherical with varied normal restitution coefficient: 1.0 (a), 0.6 (b), 0.4 (c) and 0.0 (d), particle density of 2.2 g/cm³, velocity of 10 m/s, tangent restitution coefficient of 1.0

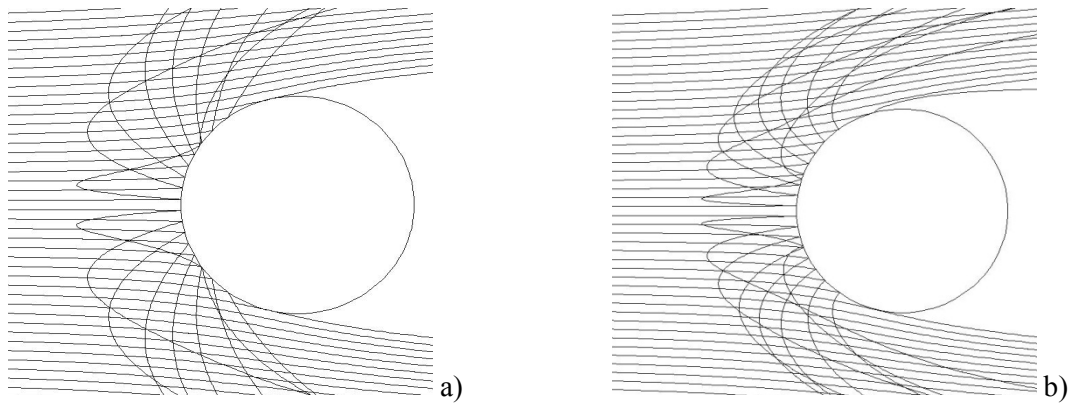


Fig. 5. Simulated trajectory for particles of 50 μm in diameter when they are spherical with varied tangent restitution coefficient: 1.0 (a), 0.4 (b), particle density of 2.2 g/cm^3 , velocity of 10 m/s, normal restitution coefficient of 1.0

In case of normal impact of ash particles, Dong et al. (2013) measured the normal restitution coefficients, in function of the incident normal velocity for particles diameter of 60 to 90 μm . The measurements were held for ash particles striking a flat steel surface. They confirmed that the coefficient depends on particle diameter and found the distribution between results large, which can result from ash composition and its plastic deformation. For instance they showed that the coefficient has its maximum of about 0.45 for incident velocity of about 2 m/s, and drops slowly to about 0.2 for velocity of 10 m/s, all in case of particles of diameter of $70 \pm 5 \mu\text{m}$. More about the theoretical and numerical approach for particle adhesion during deposition phenomenon can be found in papers by Bouris and Bertrand (1996) and Losurdo et al. (2007).

4. TRAJECTORIES OF PARTICLES STRIKING A HORIZONTAL ROW OF TUBES

After studying the trajectories of particles striking a single horizontal tube, when there is no influence of neighbouring rows, this time several predictions were done for rows of 3 horizontal tubes of 38 mm in diameter, placed in the combustion duct with a cross-flow arrangement. In front of the tube a 10 diameter long zone and behind the tube a 5 diameter zone were provided (Fig. 6). The relative tube arrangement was as follows: $s_1/D = s_2/D = 2$, one of possible convective setups. It should be pointed out that in this case the striking efficiency can be bigger than 1 owing to reflections from the side rows and tubes behind in the same row.

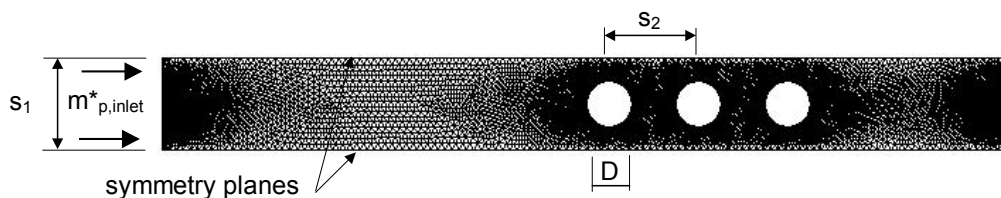


Fig. 6. Computational grid for simulations of a convective tube arrangement

The following simulations were done:

- spherical particles, with density of 2.2 g/cm^3 ;
- spherical particles, with density lowered by 25% to 1.65 g/cm^3 ;

- non-spherical particles approach with the shape factor from 1 (sphere) to 0.1 and density of 2.2 g/cm³;
- non-spherical particles with the shape factor from 1 (sphere) to 0.1 and density of 1.65 g/cm³;
- spherical particles with normal reflection coefficient from 0.1 to 0.9 and density of 2.2 g/cm³;
- spherical particles with tangent reflection coefficient from 0.1 to 0.9 and density of 2.2 g/cm³.

For all the simulations velocity of ash particles and gas entering the simulated duct was 10 m/s.

In the case of the first tube (Fig. 7) and the largest particles of 100 μm in diameter, the striking efficiency is greater than 1, for shape factors ranging from 0.4 to 1.0. It is possible only if reflections between rows of the modelled superheater cause the particles strike the surface twice or more. For particles with shape factor lower than 0.4 the striking efficiency is still greater than in case of a single tube (Fig. 2). In case of the smaller particles (50, 25 and 10 μm in diameter), the striking efficiency is almost the same as for a single tube (Fig. 2), because its inertia is too small to overcome the drag force and cross the streamlines of the gas between the rows, where its velocity increases significantly. All the results show that reflections play a major role in increasing deposit growth for in-line bundles, especially for the first, in a row, tube. The second tube in a row is hidden behind the first tube, so only bigger particles strike its surface reflecting the side rows of the tubes (Fig. 8).

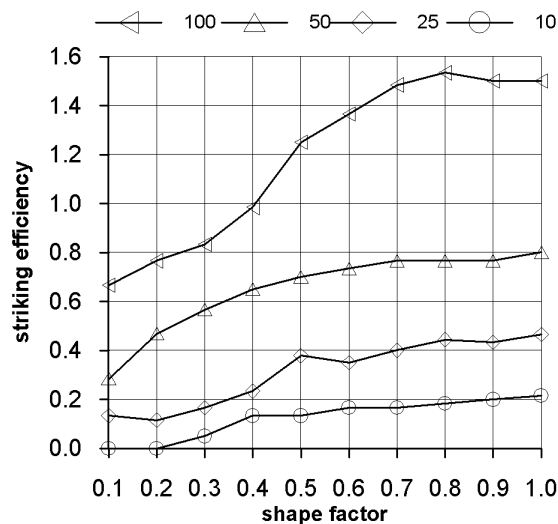


Fig. 7. Effect on striking efficiency for the first tube in a row vs. shape factor for different particle diameter (μm), particle density of 2.2 g/cm³, velocity of 10 m/s.

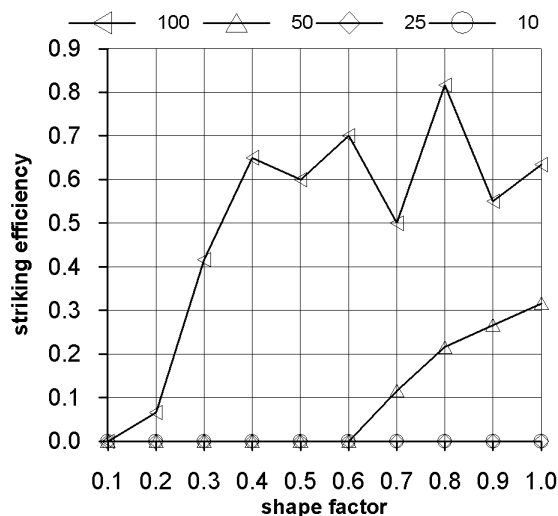


Fig. 8. Effect on striking efficiency for the second tube in a row vs. shape factor for different particle diameter (μm), particle density of 2.2 g/cm³, velocity of 10 m/s

In order to have a better understanding of the change in trajectory during the simulated impact some close-ups have been shown in Figs. 9 - 12.

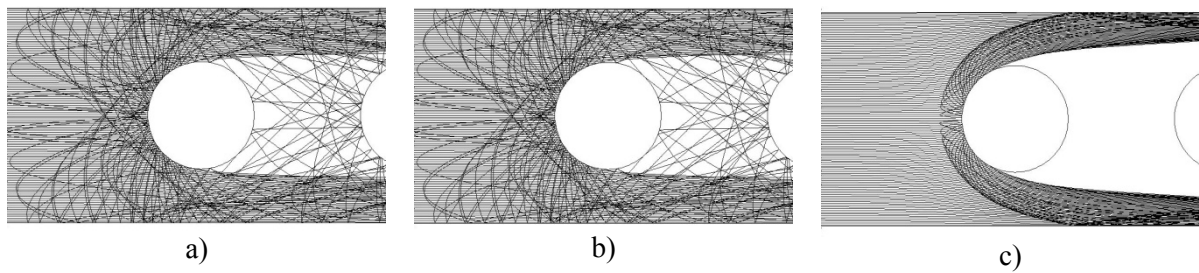


Fig. 9. Simulated trajectory for particles of 100 μm in diameter when they are spherical (a), or nonspherical with shape factor of 0.3 (b) or 0.1 (c), particle density of 2.2 g/cm^3 , velocity of 10 m/s

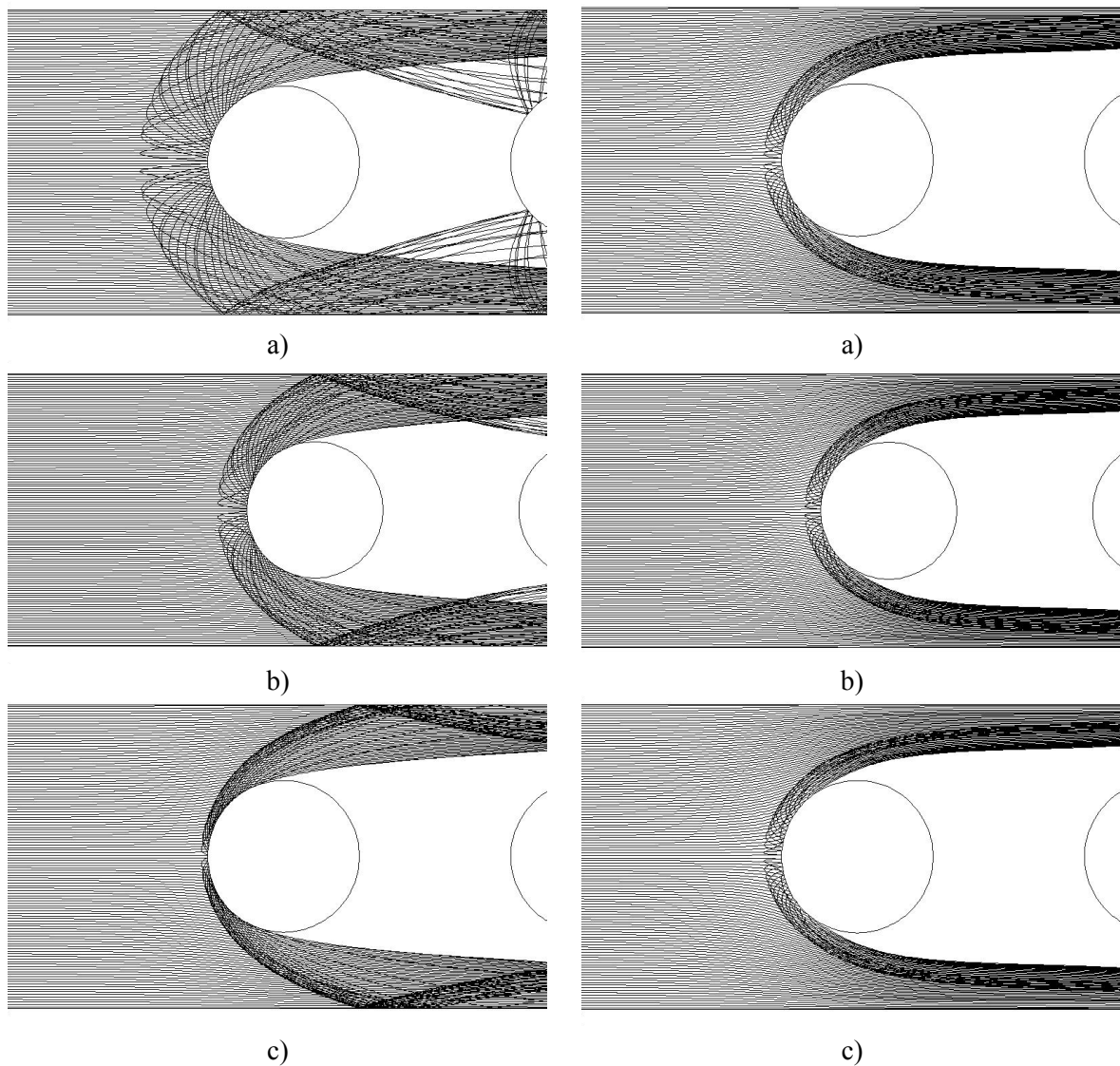


Fig. 10. Simulated trajectory for spherical particles of 50 μm in diameter when the normal restitution coefficient is 1.0 (a), or 0.5 (b) or 0.1 (c), particle density of 2.2 g/cm^3 , velocity of 10 m/s , tangent coefficient of 1.0

Fig. 11. Simulated trajectory for spherical particles of 25 μm in diameter when the tangent restitution coefficient is 1.0 (a), or 0.5 (b) or 0.1 (c), particle density of 2.2 g/cm^3 , velocity of 10 m/s , normal coefficient of 1.0

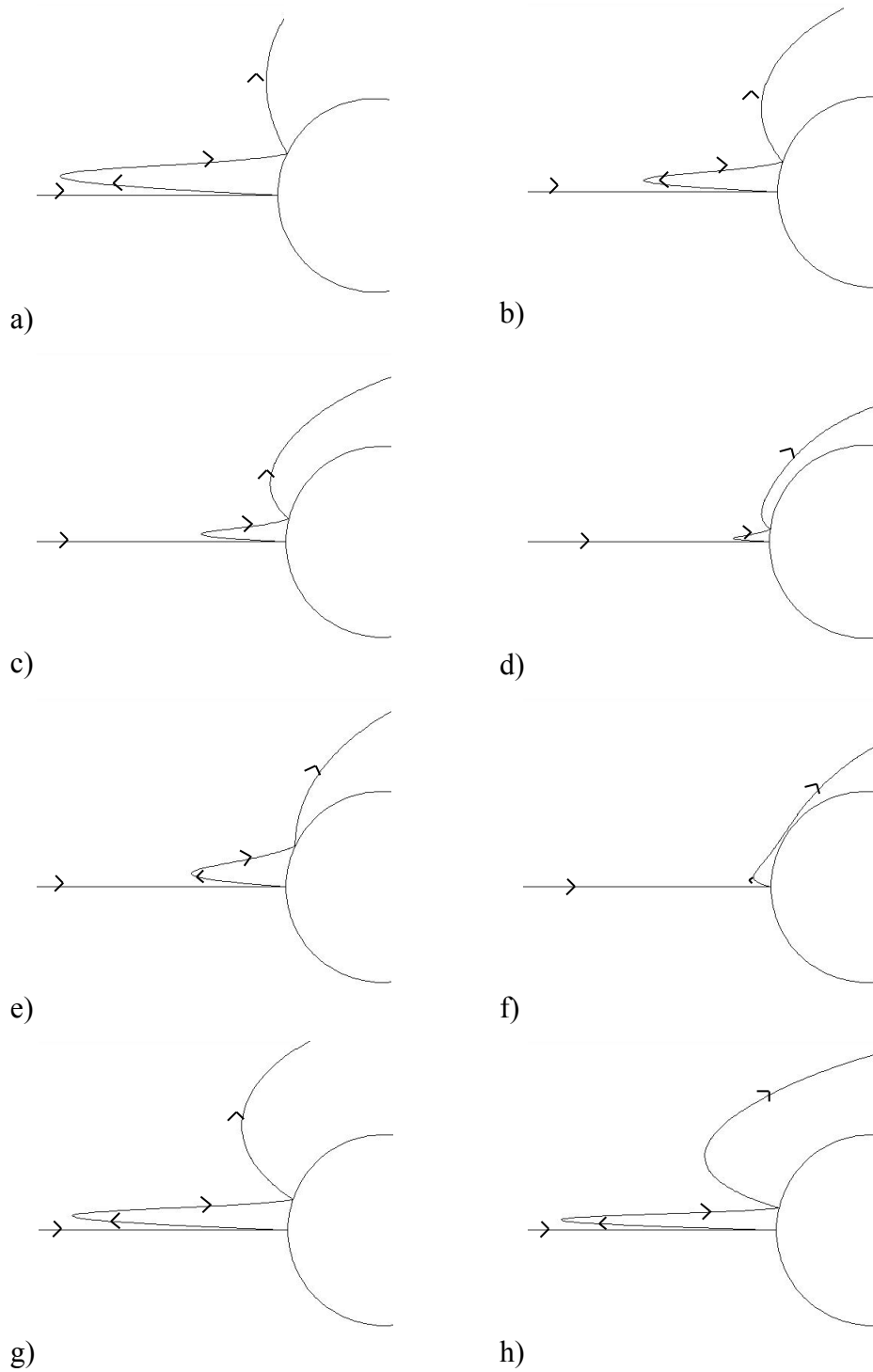


Fig. 12. Details of simulated trajectory for particles of 100 μm in diameter: spherical (a), nonspherical with shape factor of 0.5 (b), 0.3 (c) and 0.1 (d); spherical with changes in a normal restitution coefficient: 0.5 (e) or 0.1 (f); spherical with changes in a tangent restitution coefficient: 0.5 (g) or 0.1 (h); particle density of 2.2 g/cm^3 , velocity of 7.5 m/s

5. CONCLUSIONS

Constant progress in computational fluid dynamics programming enables assessing fouling of heat transfer surfaces in power boilers. An extensive body of papers on the subject published worldwide prove that the interest in using CFD code is increasing. In those cases prediction of ash particles impact onto the tube surfaces is critical. Parameters like ash particles density, their size distribution and shape factors must be determined as precisely as possible due to their significant influence on the impact phenomenon. Another set of parameters includes operational ones like velocity and temperature. The velocities of ash particles and gas particularly, decide if the particles strike the surface or not, while temperature of the gas affects its viscosity and drag force. Temperature of ash particles changes particle features, resulting in, for instance, sticking or melting or forming deposits. The third group of the parameters describes the impact in terms of momentum changes. They can influence the impact as well. Unfortunately, they are the most unknown parameters and usually are used unchanged, which means they describe elastic collision without any loss in velocity.

Investigations presented in this work were performed within the frame of the Polish Strategic Research Programme on Advanced Technologies for Power Generation (contract No.SP/E/1/67484/10).

SYMBOLS

A	area, m ²
C_D	drag coefficient
d_p	particle diameter, m
D	tube diameter, m
e_{normal}	normal restitution coefficient
e_{tangent}	tangent restitution coefficient
F_D	drag force per unit mass, m/s ²
\dot{m}_p	mass flow rate of ash particles, kg/s
$\dot{m}_{p,A}$	flux of ash particles, kg/(sm ²)
Re	Reynolds number
s_1	transverse tube spacing, m
s_2	longitudinal tube spacing, m
Stk	Stokes number
w_g	velocity of gas, m/s
w_p	velocity of ash particles, m/s

Greek symbols

η	striking (impaction) efficiency
μ_g	dynamic gas viscosity, kg/(sm)
ρ_g	density of gas, kg/m ³
ρ_p	density of ash particles, kg/m ³
ψ	correction factor for particles which do not obey Stoke's law
Φ	shape factor

Subscripts

A	surface
g	gas
i	grid element of the perimeter of a tube;
p	ash particle

REFERENCES

- Bouris D., Bergeles G., 1996. Particle-surface interactions in heat exchanger fouling. *Journal of Fluid Engineering*, 118, 574-581.
- Dong M., Li S., Xie J., Han J., 2012. Experimental Studies on the Normal Impact of Fly Ash Particles with Planar Surfaces. *Energies*, 6, 3245-3262. DOI:10.3390/en6073245.
- Epple B., Fiveland W., Krohmer B., Richards G., Benim A.C., 2005. Assessment of two-phase flow models for the simulation of pulverised coal combustion. *Clean Air: International Journal on Energy for a Clean Environment*, 6, 267-287. DOI: 10.1615/InterJEnerCleanEnv.v6.i3.50.
- Fan J.R., Zha X.D., Sun P., Cen K.F., 2001. Simulation of ash deposit in a pulverized coal-fired boiler. *Fuel*, 80, 645-654. doi.org/10.1016/S0016-2361(00)00134-4.
- Forstner M., Hohmeister G., Joller M., Dahl J., Braun M., Kleditzsch S., Schaler R., Obernberger I., 2006. CFD simulation of ash deposit formation in fixed bed biomass furnaces and boilers. *Progress in Computational Fluid Dynamics*, 6, 4/5, 248-261. DOI: 10.1504/PCFD.2006.010034.
- Haider A., Levenspiel O., 1989. Drag coefficient and terminal velocity of spherical and nonspherical particles. *Powder Techn.*, 58, 63-70. doi.org/10.1016/0032-5910(89)80008-7.
- Huang L.Y., Norman J.S., Pourkashanian M., Williams A., 1996. Prediction of ash deposition on superheater tubes from pulverized coal combustion. *Fuel*, 75, 3, 271-279. doi.org/10.1016/0016-2361(95)00220-0.
- Israel R., Rosner D.E., 1982. Use of A Generalized Stokes Number to Determine the Aerodynamic Capture Efficiency of Non-Stokesian Particles from a Compressible Gas Flow. *Aerosol Science and Technology*, 2:1, 45-51.
- Kaer S.K., Resendahl L., Adamsen P., 2001. A particle deposition model applicable to full-scale boiler simulations: sub-model testing. *Proceedings of FEDSM'01. ASME Fluids Engineering Division Summer Meeting*. New Orleans, USA, May 29-June 1, 2001, 1-6.
- Kaer S.K., Rosendahl L., Baxter L.L., 2006. Towards a CFD-based mechanistic deposition formation model for straw-fired boilers. *Fuel*, 85, 5-6, 833-848. doi.org/10.1016/j.fuel.2005.08.016.
- Lasurdo M., 2009. *Particle Tracking and Deposition from CFD Simulations using a Viscoelastic Particle Model*. PhD Thesis. TU Delft, Hollandia.
- Losurdo M., Bertrand C., Spliethoff H., 2007. A Lagrangian particle CFD post-processor dedicated to particle adhesion/deposition. *Proceedings of 7th International Conference on Heat Exchanger Fouling and Cleaning*, Tomar, Portugal, July 1 - 6.
- Lee F.C.C., Lockwood F.C., 1999. Modelling ash deposition in pulverized coal-fired applications. *Prog. Energy Combust. Sci.*, 25, 117-132. doi.org/10.1016/S0360-1285(98)00008-2.
- Ma Z., Iman F., Lu P., Sears R., Kong L., Rokanuzzman A.S., McCollor D.P., Benson S.A., 2007. A comprehensive slagging and fouling prediction tool for coal-fired boilers and its validation/application. *Fuel Processing Technology*, 88, 1035-1043. doi.org/10.1016/j.fuproc.2007.06.025
- Magda A., Magda S.I., Strelow M., Muller H., Leithner R., 2011. CFD Modelling of ash deposits in coal-fired power plants. *Proceedings of International Conference on Heat Exchanger Fouling and Cleaning-2011*. June 05-10, 2011, Crete Island, Greece.
- Morsi S.A., Alexander A.J., 1972. An investigation of particle trajectories in two-phase flow system. *J. Fluid Mech.* 55, 2, 193-208. doi.org/10.1017/S0022112072001806.
- Mueller Ch., Selenius M., Theis M., Skrifvars B.J., Backman R., Hupa M., Tran H., 2005. Deposition behaviour of molten alkali-rich fly ashes-development of a submodel for CFD applications. *Proceeding of the Combustion Institute*, 30, 2, 2991-2998. http://dx.doi.org/10.1016/j.proci.2004.08.116,
- Orłowski P., 1972. *Kotły parowe*. WNT, Warszawa, 230-234 (in Polish).
- Rushdi A., Gupta R., Sharma A., Holcombe D., 2005. Mechanistic prediction of ash deposition in a pilot-scale test facility. *Fuel*, 84, 1246-1258. DOI: 10.1016/j.fuel.2004.08.027.
- Tomeczek J., Waclawiak K., 2009. Two-dimensional modelling of deposits formation on platen superheaters in pulverized coal boilers. *Fuel*, 88, 8, 1466-1471. DOI:10.1016/j.fuel.2012.02.007.
- Waclawiak K., 2010. Numerical investigations into influence of flow direction of flue gas on formation of powder deposits onto a single horizontal tube. *Chem. Process Eng.*, 31, 2, 225-236.
- Waclawiak K., Kalisz S., 2010. Practical aspects of modeling of deposit formation from sticky ash particles at in-line superheater bundles. *Rynek energii*, 6(91), 129-134.

- Waclawiak K., Kalisz S., 2012. A practical numerical approach for prediction of particulate fouling in PC boilers. *Fuel*, 97, 38-48. doi.org/10.1016/j.fuel.2012.02.007.
- Wang H., Harb J.N., 1997. Modeling of ash deposition in large-scale combustion facilities burning pulverized coal. *Prog. Energy Combust. Sci.*, 23, 267-282. doi.org/10.1016/S0360-1285(97)00010-5.
- Weber R., Mancini M., Schaffel-Mancini N., Kupka T., 2013. On predicting the ash behaviour using Computational Fluid Dynamics. *Fuel Process. Technol.*, 105, 113-128. DOI:10.1016/j.fuproc.2011.09.008
- Weber R., Mancini N.S., Mancini M., Kupka T., 2013. Fly ash deposition modelling: Requirements for accurate predictions of particle impaction on tubes using RANS-based computational fluid dynamics. *Fuel*, 108, 586–596.
- Yang Y.B., Sharifi V.N., Swithenbank J., Ma L., Darvell L.I., Jones J.M., Pourkashanian M., Williams A., 2008. Combustion of a single particle of biomass. *Energy Fuels*, 22, 306-316. DOI: 10.1021/ef700305r.
- Yilmaz S., Cliffe K.R. 2000. Particle deposition simulation using the CFD code FLUENT. *J. Inst. Energy*, 73, 65-68.

Received 17 April 2013

Received in revised form 12 March 2014

Accepted 06 June 2014